Effects of the supersymmetric phases on the neutral Higgs sector

D. A. Demir*
The Abdus Salam International Center for Theoretical Physics, I-34100 Trieste, Italy
(Received 25 January 1999; revised manuscript received 27 May 1999; published 4 August 1999)

By using the effective potential approximation and taking into account the dominant top quark and scalar top quark loops, radiative corrections to the MSSM Higgs potential are computed in the presence of the supersymmetric *CP*-violating phases. It is found that the lightest Higgs scalar remains essentially *CP* even as in the *CP*-invariant theory whereas the other two scalars are heavy and do not have definite *CP* properties. The supersymmetric *CP*-violating phases are shown to modify significantly the decay rates of the scalar to fermion pairs. [S0556-2821(99)08113-8]

PACS number(s): 12.60.Jv, 11.30.Er, 12.60.Fr

I. INTRODUCTION

The minimal supersymmetric standard model (MSSM) consists of various soft-supersymmetry-breaking parameters as well as the Higgsino mass parameter μ coming from the superpotential. In general, there is no *a priori* reason for taking all these parameters to be real, and thus, Yukawa couplings, gaugino masses, trilinear Higgs-boson–sfermion couplings, A_f, Higgs boson bilinear coupling, $m_3^2 \equiv \mu B$, and μ parameter themselves can all be complex. On the other hand, the MSSM Lagrangian has two global symmetries $\mathrm{U}(1)_{PQ}$ (Peccei-Quinn symmetry) and $\mathrm{U}(1)_{R\text{-}PQ}$ (an R symmetry) under which all fields and parameters are charged. The selection rules for these symmetries limit the combinations of dimensionful parameters that can appear in a physical quantity so that one has, in fact, only three of these phases as physical [1,2]. Without loss of generality, these three physical phases can be identified with (1) the phase in the Cabibbo-Kobayashi-Maskawa matrix δ_{CKM}, (2) $\varphi_\mu \equiv \mathrm{Arg}(\mu)$, and (3) $\varphi_{A_f} \equiv \mathrm{Arg}(A_f)$. Thus any physical quantity $\mathcal{F}$ has an explicit dependence on these phases: $\mathcal{F} = \mathcal{F}(\delta_{CKM}, \varphi_\mu, \varphi_{A_f})$.

Despite their presence in the Lagrangian, the phenomenological relevance of these *CP*-violating phases has often been questioned due to the smallness of the neutron and electron electric dipole moments [1,3] which require them to be at most $\mathcal{O}(10^{-3})$. However, recent studies have shown that it is possible to suppress neutron and electron dipole moments without requiring these *CP*-violating phases be small by allowing the existence of either nonuniversal soft breaking parameters at the unification scale [4], some kind of cancellation among various supersymmetric contributions [5], or heavy enough sfermions for the first two generations [6]. In fact, following the last scenario, it was recently shown that the *CP* violation in B and K systems can be saturated with φ_μ and φ_{A_f} only [7]. Apart from electric dipole moments and weak decays, these phases play a crucial role in the creation of the baryon asymmetry of the universe at the electroweak phase transition [8].

In this work, assuming that the electric dipole moments are suppressed by one of the methods metioned above, we take supersymmetric phases to be unconstrained and investigate their effects on the Higgs sector of the MSSM. At the tree level the Higgs sector of the MSSM conserves *CP* due to the fact that the superpotential is holomorphic in superfields entailing the absence of flavor-changing neutral currents and scalar-pseudoscalar mixings. When the supersymmetric phases φ_μ and φ_{A_f} vanish the Higgs sector conserves *CP* at any loop order. In fact, the *CP*-conserving Higgs sector has been analyzed by several authors with the main purpose of evaluating the mass of the lightest Higgs boson which has the tree-level upper bound of M_Z. It has been found that radiative corrections, dominated by top quark and top squark loops, elevate the tree-level bound significantly [9]. These one-loop results [9] have been improved by utilizing complete one-loop on-shell renormalization [10], renormalization group methods [11], diagrammatic methods with leading order QCD corrections [12], and two-loop on-shell renormalization [13]. However, when the supersymmetric phases are nonvanishing, as recent studies have shown [14], the Higgs sector becomes *CP* violating through radiative corrections. As in the *CP*-conserving case, the radiative corrections will be dominated by the top quark and top squark loops. Below we investigate effects of the supersymmetric phases on the Higgs boson masses, scalar-pseudoscalar mixings, and decay properties of scalars to fermion pairs. In doing this, we shall calculate one-loop radiative corrections coming from top quark and top squark loops in the effective potential approximation.

This work is organized as follows. In Sec. II we compute the one-loop effective potential using top quark and top squark contributions together with the specification of the particle spectrum and mixings. In Sec. III we discuss, as an example, the decay properties of the Higgs scalars to fermion pairs. In Sec. IV we conclude the work.

II. EFFECTIVE POTENTIAL

The Higgs sector of the MSSM consists of two SU(2) doublets H_1, H_2, with opposite hypercharges $Y_1 = -1$, $Y_2 = +1$, and nonvanishing vacuum expectation values v_1, v_2. Allowing a finite alignment θ between the two Higgs doublets, we adopt the following decomposition:

*Email address: ddemir@ictp.trieste.it

$$H_1=\begin{pmatrix} H_1^0 \\ H_1^- \end{pmatrix}=\frac{1}{\sqrt{2}}\begin{pmatrix} v_1+\phi_1+i\varphi_1 \\ H_1^- \end{pmatrix},$$

$$H_2=\begin{pmatrix} H_2^+ \\ H_2^0 \end{pmatrix}=\frac{e^{i\theta}}{\sqrt{2}}\begin{pmatrix} H_2^+ \\ v_2+\phi_2+i\varphi_2 \end{pmatrix}. \quad (1)$$

At the tree level the Higgs sector is described by the scalar potential

$$V_0(H_1,H_2)=m_1^2|H_1|^2+m_2^2|H_2|^2+(m_3^2 H_1\cdot H_2+\text{H.c.}) + \frac{\lambda_1}{2}|H_1|^4+\frac{\lambda_2}{2}|H_2|^4+\lambda_{12}|H_1|^2|H_2|^2 + \tilde{\lambda}_{12}|H_1\cdot H_2|^2, \quad (2)$$

with the parameters

$$m_1^2=m_{\tilde{H}_1}^2+|\mu|^2, \quad m_2^2=m_{\tilde{H}_2}^2+|\mu|^2, \quad m_3^2=|\mu B|,$$

$$\lambda_1=\lambda_2=(g_2^2+g_1^2)/4, \quad \lambda_{12}=(g_2^2-g_1^2)/4, \quad \tilde{\lambda}_{12}=-g_2^2/2, \quad (3)$$

where $m_{\tilde{H}_{1,2}}^2$ and B are the soft-supersymmetry-breaking parameters. As is seen from Eqs. (3), the tree-level potential is described by real parameters; thus, the alignment between the two doublets can, in fact, be rotated away. Since, in the minimum, the potential is to have vanishing gradients in all directions, in particular, $\partial V_0/\partial\varphi_{1,2}=m_3^2\sin\theta=0$, one automatically gets $\theta=0$. Those terms of the tree-level potential (2) quadratic in the components of the Higgs doublets (1) give the mass-squared matrix of neutral scalars the diagonalization of which yields the $CP=-1$ boson $A^0=\cos\beta\varphi_1-\sin\beta\varphi_2$ with mass $M_{A^0}^2=-m_3^2/\sin\beta\cos\beta$, and two $CP=+1$ bosons which are linear combinations of ϕ_1 and ϕ_2 with a mixing angle α. The mixing angle α and the masses of the CP even scalars h and H are given by [15]

$$\tan 2\alpha=\frac{M_{A^0}^2+M_Z^2}{M_{A^0}^2-M_Z^2}\tan 2\beta, \quad (4)$$

$$M_{h(H)}^2=\frac{1}{2}[M_{A^0}^2+M_Z^2-(+) \times\sqrt{(M_{A^0}^2+M_Z^2)^2-4M_{A^0}^2M_Z^2\cos^2 2\beta}], \quad (5)$$

where $\tan\beta\equiv v_2/v_1$, and $M_Z^2=(g_2^2+g_1^2)(v_1^2+v_2^2)/4$ in our convention. It is readily seen that for $\tan\beta\gtrsim 2$ one has $\beta\sim\pi/2$, $M_h\sim M_Z$, and $M_H\sim M_A$. However, it is known that radiative corrections elevate M_h (bounded by M_Z at the tree level) significantly [9] without modifying the mass degeneracy between H and A when the theory conserves CP. When, however, the CP-violating MSSM phases are switched on, the degeneracy between H and A can be lifted considerably as discussed in [14].

We now start computing the radiative corrections to the tree potential (2) in the presence of the CP-violating MSSM phases φ_{μ,A_f}. Our main concern will be the investigation of the masses and mixings of the scalars as a function of the CP-violating angles. These mixings could be CP conserving (such as h-H mixing in the CP-respecting limit) as well as CP violating as we will discuss below. To evaluate the radiative corrections we follow the effective potential approximation where the tree-level potential (2) is added to the one-loop contributions having the famous Coleman-Weinberg [9,16] form

$$\Delta V=\frac{1}{64}\text{Str}\,\mathcal{M}^4(H_1,H_2)\left(\log\frac{\mathcal{M}^2(H_1,H_2)}{Q^2}-\frac{3}{2}\right), \quad (6)$$

where $\text{Str}\equiv\Sigma_J(-1)^{2J+1}(2J+1)\text{Tr}$ is the usual supertrace, and $\mathcal{M}(H_1,H_2)$ is the Higgs-field-dependent mass matrix of particles. ΔV depends on the renormalization scale Q which is presumably around the weak scale. In evaluating ΔV one includes the contributions of vector bosons, Higg bosons, and fermions as well as their supersymmetric partners gauginos, Higgsinos, and sfermions. Among all these particles top quarks and scalar top quarks give the dominant contributions [9]. However, for very large $\tan\beta$ values bottom-quark–bottom-squark and τ-stau systems can become important. In addition to these, since the dependence of ΔV on the CP-violating phases φ_{μ,A_f} originates from only the Higgsino (through μ dependence) and sfermion (through μ and A_f dependence) mass matrices, these two particle species attain a separate importance. However, if one wishes to include Higgsino contributions, all particle species must be included since then the precision of computation rises to the level of gauge couplings. In the following we neglect the contributions of gauge couplings and restrict ourselves to moderate values of $\tan\beta$ so that, to a good approximation, the dominant terms in ΔV are given by top-quark–top-squark system. This approximation is convenient in that it picks up the phase-sensitive dominant contributions to ΔV.

In the $(\tilde{t}_L,\tilde{t}_R)$ basis the top-squark mass-squared matrix, neglecting the D-term contributions, takes the form

$$M_{\tilde{t}}=\begin{pmatrix} M_{\tilde{L}}^2+h_t^2|H_2^0|^2 & h_t(A_tH_2^0-\mu^*H_1^{0*}) \\ h_t(A_t^*H_2^{0*}-\mu H_1^0) & M_{\tilde{R}}^2+h_t^2|H_2^0|^2 \end{pmatrix}, \quad (7)$$

where μ and A_t are complex, $M_{\tilde{L},\tilde{R}}^2$ are the soft masses squared of left- and right-handed top squarks, and h_t is the top Yukawa coupling. Denoting the eigenvalues of $M_{\tilde{t}}$ by $m_{\tilde{t}_{1,2}}^2$ and using $m_t^2=h_t^2|H_2^0|^2$ the one-loop effective potential takes the form

$$V=V_0+\frac{6}{64\pi^2}\left[\sum_{a=\tilde{t}_1,\tilde{t}_2} m_a^4\left(\log\frac{m_a^2}{Q^2}-\frac{3}{2}\right) - 2m_t^4\left(\log\frac{m_t^2}{Q^2}-\frac{3}{2}\right)\right]. \quad (8)$$

We require this effective potential be minimized at (v_1,v_2,θ) at which it has to have vanishing gradients in all

directions and the masses of the Higgs scalars must be real positive. Gradients of the potential with respect to the charged components of the Higgs doublets automatically vanish as there are no charge-breaking effects in the vacuum. On the other hand, extremization of V with respect to neutral components of the Higgs doublets yields

$$v_1[2m_1^2+\lambda_1 v_1^2+(\lambda_{12}+\tilde{\lambda}_{12})v_2^2]+2m_3^2 v_2\cos\theta+2\left(\frac{\partial\Delta V}{\partial\phi_1}\right)_0=0, \tag{9}$$

$$v_2[2m_2^2+\lambda_2 v_2^2+(\lambda_{12}+\tilde{\lambda}_{12})v_1^2]+2m_3^2 v_1\cos\theta+2\left(\frac{\partial\Delta V}{\partial\phi_2}\right)_0=0, \tag{10}$$

$$m_3^2 v_2\sin\theta-\left(\frac{\partial\Delta V}{\partial\varphi_1}\right)_0=0, \tag{11}$$

$$m_3^2 v_1\sin\theta-\left(\frac{\partial\Delta V}{\partial\varphi_2}\right)_0=0, \tag{12}$$

where the subscript ''0'' implies the substitution $\phi_1=\phi_2=\varphi_1=\varphi_2=0$ in the corresponding quantity. Equations (9) and (10) come as no surprise as they are the counterparts of the ones occurring in the *CP*-conserving case. However, with $(\partial\Delta V/\partial\varphi_{1,2})_0\neq 0$, Eqs. (11) and (12) now imply a nontrivial solution for $\sin\theta$ unlike the *CP*-conserving case where these gradients indentically vanish and one automatically obtains a vanishing θ. After some algebra one can show that

$$\left(\frac{\partial\Delta V}{\partial\varphi_1}\right)_0=\tan\beta\left(\frac{\partial\Delta V}{\partial\varphi_2}\right)_0. \tag{13}$$

Therefore, Eqs. (11) and (12) imply one and the same solution for θ,

$$m_3^2\sin\theta=\frac{1}{2}\beta_{h_t}|\mu||A_t|\sin\gamma f(m_{\tilde{t}_1}^2,m_{\tilde{t}_2}^2), \tag{14}$$

where $\beta_{h_t}=3h_t^2/16\pi^2$, $\gamma=\varphi_\mu+\varphi_{A_t}$, and

$$f(x,y)=-2+\log\frac{xy}{Q^4}+\frac{y+x}{y-x}\log\frac{y}{x} \tag{15}$$

is a scale-dependent one-loop function. Actually, if one uses the decomposition of the Higgs doublets in Eqs. (1), in all one-loop formula γ gets replaced by $\gamma+\theta$. However, since θ itself is a loop-induced quantity, its appearance together with γ is a two- and higher-loop effect which we neglect. Thus, when computing ΔV we drop θ from Eqs. (1), knowing that it is induced through Eq. (14). It is readily seen from Eq. (14) that unless γ vanishes θ remains finite. Furthermore, as a result of the form of the top-squark mass-squared matrix, all one-loop quantities turn out to depend on the combination $\gamma=\varphi_\mu+\varphi_{A_t}$. Of course, had we included Higgsino contributions there would be terms that depend solely on φ_μ, destructing this kind of relation. However, they would be subleading compared to the top quark and top squark contributions discussed here.

In Eq. (14) and all formulas below $m_{\tilde{t}_{1,2}}^2$ denote top-squark mass-squared eigenvalues evaluated at the minimum of the potential:

$$m_{\tilde{t}_{1,2}}^2=\frac{1}{2}(M_{\tilde{L}}^2+M_{\tilde{R}}^2+2m_t^2\mp\Delta_{\tilde{t}}^2), \tag{16}$$

where

$$\Delta_{\tilde{t}}^2=\sqrt{(M_{\tilde{L}}^2-M_{\tilde{R}}^2)^2+4m_t^2(|A_t|^2+|\mu|^2\cot^2\beta-2|\mu||A_t|\cot\beta\cos\gamma)}. \tag{17}$$

As usual, construction of the mass-squared matrix of the Higgs scalars proceeds through the evaluation of

$$M^2=\left(\frac{\partial^2 V}{\partial\chi_i\partial\chi_j}\right)_0,\quad \text{where}\quad \chi_i\in\mathcal{B}=\{\phi_1,\phi_2,\varphi_1,\varphi_2\}. \tag{18}$$

Solving $m_{1,2}^2$ from the extremization conditions (9) and (10), and replacing them in M^2, one observes that, in the basis $\mathcal{B}$, the vector $\{0,0,\cos\beta,-\sin\beta\}$ corresponds to the Golstone mode G^0 absorbed by Z bosons to acquire its mass. Then in the reduced basis $\mathcal{B}'=\{\phi_1,\phi_2,\sin\beta\varphi_1+\cos\beta\varphi_2\}$ the mass-squared matrix of the Higgs scalars becomes

$$M^2=\begin{pmatrix} M_Z^2c_\beta^2+\tilde{M}_A^2s_\beta^2+\Delta_{11} & -(M_Z^2+\tilde{M}_A^2)s_\beta c_\beta+\Delta_{12} & r\Delta \\ -(M_Z^2+\tilde{M}_A^2)s_\beta c_\beta+\Delta_{12} & M_Z^2s_\beta^2+\tilde{M}_A^2c_\beta^2+\Delta_{22} & s\Delta \\ r\Delta & s\Delta & \tilde{M}_A^2+\Delta \end{pmatrix}, \tag{19}$$

where $c_\beta=\cos\beta$ and $s_\beta=\sin\beta$. The scalar mass-squared matrix involves various parameters whose explicit expressions we list below. The adimensional parameters r and s are given by

$$r=-\frac{\sin\beta}{\sin\gamma}\frac{|A_t|\cos\gamma-|\mu|\cot\beta}{|A_t|}, \tag{20}$$

$$s=\frac{\sin\beta}{\sin\gamma}\frac{1}{|\mu||A_t|g(m^2_{\tilde t_1},m^2_{\tilde t_2})}\left(|A_t|(|A_t|-|\mu|\cot\beta\cos\gamma)g(m^2_{\tilde t_1},m^2_{\tilde t_2})-(m^2_{\tilde t_2}-m^2_{\tilde t_1})\log\frac{m^2_{\tilde t_2}}{m^2_{\tilde t_1}}\right). \tag{21}$$

While r originates mainly from the top-squark left-right mixings, s has an additional term depending on the the top squark mass splitting $\log(m^2_{\tilde t_2}/m^2_{\tilde t_1})$.

The parameters of mass dimension can be expressed as follows:

$$\Delta=-\beta_{h_t}\frac{\sin^2\gamma}{\sin^2\beta}\frac{|\mu|^2|A_t|^2m_t^2}{(m^2_{\tilde t_2}-m^2_{\tilde t_1})^2}g(m^2_{\tilde t_1},m^2_{\tilde t_2}), \tag{22}$$

$$\Delta_{11}=-2\beta_{h_t}\frac{|\mu|^2m_t^2(|A_t|\cos\gamma-|\mu|\cot\beta)^2}{(m^2_{\tilde t_2}-m^2_{\tilde t_1})^2}g(m^2_{\tilde t_1},m^2_{\tilde t_2}), \tag{23}$$

$$\Delta_{12}=-2\beta_{h_t}|\mu|m_t^2\left\{\frac{|A_t|\cos\gamma-|\mu|\cot\beta}{(m^2_{\tilde t_2}-m^2_{\tilde t_1})}\log\frac{m^2_{\tilde t_2}}{m^2_{\tilde t_1}}-\frac{|A_t|[(|A_t|\cos\gamma-|\mu|\cot\beta)^2+|A_t|(|A_t|-|\mu|\cot\beta)\sin^2\gamma]}{(m^2_{\tilde t_2}-m^2_{\tilde t_1})^2}g(m^2_{\tilde t_1},m^2_{\tilde t_2})\right\}, \tag{24}$$

$$\Delta_{22}=2\beta_{h_t}m_t^2\left\{\log\frac{m^2_{\tilde t_2}m^2_{\tilde t_1}}{m_t^4}+\frac{2|A_t|(|A_t|-|\mu|\cot\beta\cos\gamma)}{(m^2_{\tilde t_2}-m^2_{\tilde t_1})}\log\frac{m^2_{\tilde t_2}}{m^2_{\tilde t_1}}-\frac{|A_t|^2(|A_t|-|\mu|\cot\beta\cos\gamma)^2}{(m^2_{\tilde t_2}-m^2_{\tilde t_1})^2}g(m^2_{\tilde t_1},m^2_{\tilde t_2})\right\}, \tag{25}$$

where the function $g(m^2_{\tilde t_1},m^2_{\tilde t_2})$ in these expressions reads

$$g(x,y)=f(x,y)-\log\frac{xy}{Q^4}. \tag{26}$$

Therefore, unlike $f(m^2_{\tilde t_1},m^2_{\tilde t_2})$, $g(m^2_{\tilde t_1},m^2_{\tilde t_2})$ does not have an explicit dependence on the renormalization scale Q. In fact, the adimensional parameters r and s as well as the mass parameters (21)–(24) have no explicit dependence on Q. On the other hand, the remaining mass parameter $\tilde M_A^2$ in the scalar mass-squared matrix (19) is an explicit function of Q:

$$\tilde M_A^2=\frac{m_3^2}{\sin\beta\cos\beta}\frac{\sin(\theta-\gamma)}{\sin\gamma}. \tag{27}$$

It is the θ, Eq. (13), dependence of $\tilde M_A^2$ that makes it Q dependent. However, the explicit Q dependence of θ should cancel with the implicit Q dependence of $\tan\beta$ and m_3^2 to make $\tilde M_A^2$ scale independent [9].

According to the decomposition of Higgs doublets in Eqs. (1), ϕ_1 and ϕ_2 are of $CP=+1$ whereas $\sin\beta\varphi_1+\cos\beta\varphi_2$ is of $CP=-1$. As suggested by the form of the scalar mass-squared matrix (19) there are mainly two kinds of mixings: (1) mixing of the scalars with different CP induced by $M_{13}^2=r\Delta$ and $M_{23}^2=s\Delta$, and (2) mixing of the $CP=+1$ scalars through $M_{12}^2=-(M_Z^2+\tilde M_A^2)s_\beta c_\beta+\Delta_{12}$. While the former are induced purely by the nonvanishing supersymmetric phases the latter exist in the CP-respecting limit too. When the CP-violating phases vanish, that is, $\gamma\to0$, one gets $r\Delta\to0$, $s\Delta\to0$, and $\Delta\to0$. In this case $CP=+1$ and $CP=-1$ sectors in Eq. (19) decouple and reproduce the particle spectrum of the CP-conserving limit in which $\tilde M_A$ becomes the radiatively corrected pseudoscalar mass and $\Delta_{11,12,22}$ become usual the one-loop contributions [9] to the $CP=+1$ scalar mass-squared matrix. For a proper interpretation of results of the numerical analysis below it is convenient to know the relative strengths of the CP-violating and -conserving mixings. For large $\tan\beta$, Eqs. (20) and (21) go over to

$$r\sim-\sin\beta\cot\gamma,\quad s\sim\frac{\sin\beta}{\sin\gamma}\left(\frac{|A_t|}{|\mu|}+\frac{4(m_t^2+M_Q^2)}{|\mu||A_t|}\right), \tag{28}$$

where we assumed $M_{\tilde L}\sim M_{\tilde R}\equiv M_Q^2\gg m_t|A_t|$ and $|A_t|\gg|\mu|\cot\beta$ in the derivation. Equation (28) implies that $|r|/s\ll1$. This follows mainly from the dependence of the top squark mass matrix (7) on H_2^0 which causes not only $|s\Delta|$ but also $|\Delta_{12}|$ and $|\Delta_{22}|$ to be larger than $|\Delta_{11}|$ and $|r\Delta|$ through top squark and top-squark–top-quark top splittings. An immediate consequence of Eqs. (28) is that one eigenstate of the scalar mass-squared matrix (19) will be of mainly $CP=+1$. Thus one expects that among the three mass eigenstate scalars one will continue to have $CP=+1$ with a small $CP=-1$ component while the other two can mix significantly depending on the relative strengths of the other one-loop corrections. This observation can be justified numerically by analyzing the relative strengths of CP-violating and CP-conserving mixings as classified above. Figure 1

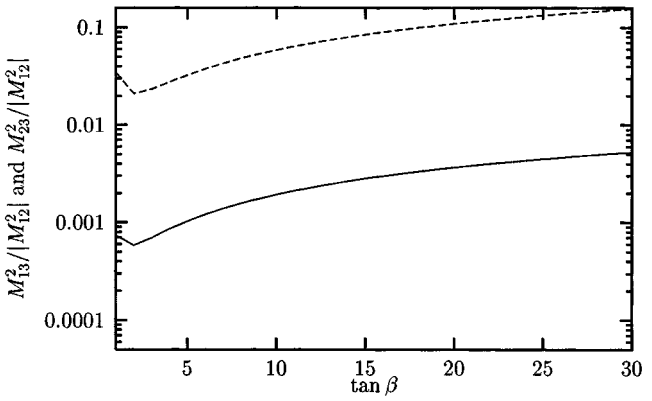

FIG. 1. Variation of $M_{13}^2/|M_{12}^2|$ (solid curve) and $M_{23}^2/|M_{12}^2|$ (dashed curve) with $\tan\beta$ for $M_{\tilde{L}}=M_{\tilde{R}}=|A_t|=10M_Z$, $|\mu|=2.5M_Z$, and $\tilde{M}_A=2M_Z$ with $\gamma=\pi/4$. The *CP*-violating mixings become important for large $\tan\beta$.

shows the variation of $M_{13}^2/|M_{12}^2|$ (solid curve) and $M_{23}^2/|M_{12}^2|$ (dashed curve) with $\tan\beta$ for $M_{\tilde{L}}=M_{\tilde{R}}=|A_t|=10M_Z$, $|\mu|=2.5M_Z$, and $\tilde{M}_A=2M_Z$ with $\gamma=\pi/4$. As the figure suggests, the larger the $\tan\beta$, the larger the *CP*-violating mixings compared to the mixing between the $CP=+1$ components. The increase of these ratios with $\tan\beta$ can be understood as follows: (1) $\beta\to\pi/2$ as $\tan\beta$ grows to higher values, and thus, $|-(M_Z^2+\tilde{M}_A^2)s_\beta c_\beta|$ decreases gradually; (2) Δ_{12} is positive for these parameters (and even for higher values of $|\mu|$ due to $\cot\beta$ suppression) and grows with $\tan\beta$ due to $\log m_{\tilde{t}_2}^2/m_{\tilde{t}_1}^2$ so that M_{12}^2 decreases with increasing $\tan\beta$, and the ratios increase gradually since M_{13}^2 and M_{23}^2 decrease with $\tan\beta$ more slowly.

In Fig. 1 we plot ratios of the *CP*-violating mixings to *CP*-conserving ones; however, if one plots *CP*-violating mixings directly, for example in units of $(10M_Z)^2$ for $|\mu|=10M_Z$, $\gamma=\pi/2$, and $\tilde{M}_A=5M_Z$, in absolute magnitude, $M_{13}^2(M_{23}^2)$ starts with $\sim 4\times 10^{-2}(\sim 10^{-2})$ at $\tan\beta=2$ and falls down $3\times 10^{-5}(2\times 10^{-4})$ at $\tan\beta\sim 30$. These results generally agree with those of [14] though the computational schemes are different.

Since the parameter space is too wide to cover fully, in the following we restrict ourselves to the following set:

$$M_{\tilde{L}}=M_{\tilde{R}}=500\ \text{GeV},\quad |A_t|=1\ \text{TeV},$$
$$|\mu|=250\ \text{GeV},\quad \tilde{M}_A=200\ \text{GeV}, \tag{29}$$

and vary γ over its full range. Each time we consider low- and high-$\tan\beta$ regimes separately by taking $\tan\beta=4$ and 30. As $\tan\beta$ increases $|\mu|\cot\beta$ decreases, and this enhances the contribution of the radiative corrections. However, variation with $\tan\beta$ is not the whole story because even for $\cot\beta\rightsquigarrow 0$, Δ, Δ_{11}, Δ_{12} are proportional to $|\mu||A_t|$ so that choice for the latter affects the strength of the radiative corrections. Especially for large $\tan\beta$, top squark masses weakly depend on $|\mu|$; therefore, these elements of the mass-squared matrix become more sensitive to the choice for $|\mu|$. The parameter set (29) is a moderate choice in that it enhances the radiative corrections through a large $|A_t|$ term without causing too big splittings among the Δ coefficients in Eqs. (22)–(25) thanks to the relatively small $|\mu|$ term. Dependence on the parameter $\tilde{M}_A$ is as in the *CP*-invariant theory, namely, heavy scalars have masses around $\tilde{M}_A$.

In principle one can diagonalize analytically the scalar mass-squared matrix (19); however, the results will be too complicated to be suggestive. Instead of using such oblique expressions we shall fix the notation for diagonalization and numerically analyze the results. The scalar mass-squared matrix (19) can be diagonalized by a similarity transformation

$$\mathcal{R}\cdot M^2\cdot\mathcal{R}^T=\text{diag}(M_{H_1}^2,M_{H_2}^2,M_{H_3}^2),\quad \text{where}\quad \mathcal{R}\cdot\mathcal{R}^T=1, \tag{30}$$

where the mass-eigenstate scalar fields are defined by

$$\begin{pmatrix} H_1\\ H_2\\ H_3\end{pmatrix}=\mathcal{R}\begin{pmatrix}\phi_1\\ \phi_2\\ \sin\beta\varphi_1+\cos\beta\varphi_2\end{pmatrix}. \tag{31}$$

γ dependence of the elements of $\mathcal{R}$ is crucial for determining the *CP* impurity of the mass eigenstate scalars H_i. In analyzing $\mathcal{R}$ we adopt a convention such that in the limit of vanishing γ we let $H_1\to h$, $H_2\to H$, and $H_3\to A$; that is, H_1 is the lightest Higgs boson. We expect the results of the *CP*-invariant theory to be recovered at the *CP*-conserving points $\gamma=0,\ \pi,\ 2\pi$ except for the γ dependence of various parameters.

Depicted in Fig. 2 is the γ dependence of the H_1 composition in percent for the parameter set in Eq. (29). From the left panel we observe that, on the average, H_1 has $\sim 30\%$ ϕ_1 and $\sim 70\%$ ϕ_2 composition. As is noticed immediately from the figure, the $CP=-1$ component of H_1 is small, in fact, it never exceeds 0.02% in the entire range of γ. From the right panel, however, we observe that the ϕ_2 contribution rises near to the 100% line, and correspondingly, the ϕ_1 contribution remains below 2.5%. This result is a consequence of the $\beta\to\pi/2$ limit reminiscent from the *CP*-invariant theory. In this large $\tan\beta$ limit, the $\sin\beta\varphi_1+\cos\beta\varphi_2$ composition of H_1 reaches at most of 0.2% over the entire range of γ. It is clear that both windows of the figure suggests that the lightest Higgs boson remains essentially a *CP*-even Higgs scalar for the parameter space in Eq. (29).

In Fig. 3 we show the percentage composition of H_2 as a function of γ for $\tan\beta=4$ (left panel) and $\tan\beta=30$ (right panel). In agreement with the left panel of Fig. 2, for $\tan\beta=4$ (left panel) H_2 has $\sim 70\%$ ϕ_1 and $\sim 30\%$ ϕ_2 composition. Unlike H_1, however, the $\sin\beta\varphi_1+\cos\beta\varphi_2$ composition of H_2 becomes as large as 1.3%. As expected, this increase in the $CP=-1$ component is compensated by H_3. A more spectacular side of Fig. 3 arises for large $\tan\beta$ (right panel) in which H_2 is seen to gain non-negligible *CP*-odd composition. In accordance with the large $\tan\beta$ limit described by Eq. (28) there is a strong dependence γ. The sum of the ϕ_1 and ϕ_2 compositions of H_2 starts from $\gamma=0$ at the 100% line, and the former is diminished rather fast until $\gamma=\pi/2$. Beyond this point it rises rapidly to the 98% line at $\gamma=\pi$ where its

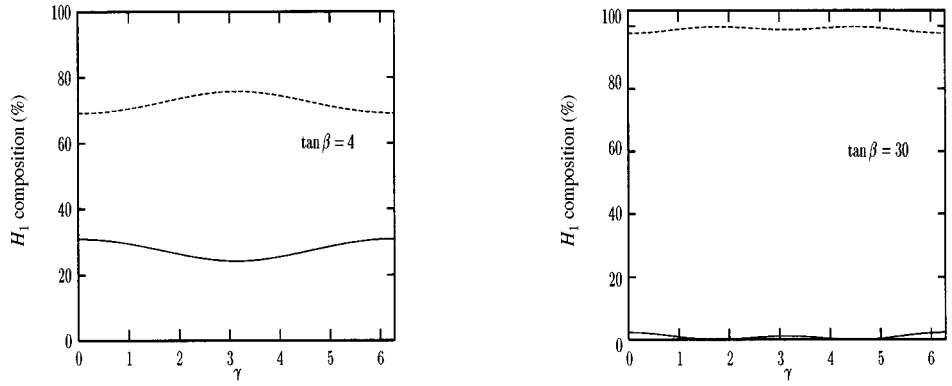

FIG. 2. Percentage composition of H_1 as a function of γ for $\tan\beta=4$ (left panel) and $\tan\beta=30$ (right panel). Here ϕ_1, ϕ_2, and $\sin\beta\varphi_1+\cos\beta\varphi_2$ contributions are $|\mathcal{R}_{11}|^2$ (solid curve), $|\mathcal{R}_{12}|^2$ (dashed curve), and $|\mathcal{R}_{13}|^2$ (short-dashed curve), in percents. Values of the parameters are given in Eqs. (29).

$CP=+1$ component completes to 100% in accordance with the CP conservation. One notes the complementary behavior of the $\sin\beta\varphi_1+\cos\beta\varphi_2$ composition which, in particular, implies that H_2 is a pure pseudoscalar around $\gamma=\pi/2$.

Depicted in Fig. 4 is the percentage composition of H_3 as a function of γ for $\tan\beta=4$ (left panel) and $\tan\beta=30$ (right panel). In agreement with the left panels of Figs. 2 and 3, H_3 is almost a pure pseudoscalar for $\tan\beta=4$. On the other hand, for $\tan\beta=30$ (right panel) H_3 is seen to lose its CP purity in accordance with the right panel of Fig. 3. Thus H_3, except for the points discussed above, does not have definite CP characteristics. From Figs. 3 and 4 one concludes that heavy scalars have non-negligible CP impurity in agreement with the results of [14].

ϕ_1 (solid curve), ϕ_2 (dashed curve), and $\sin\beta\varphi_1+\cos\beta\varphi_2$ (short-dashed curve) compositions of the Higgs field H_i shown in Figs. 2–4 need further elaboration. In accordance with Fig. 1, CP-violating mixings are small for small $\tan\beta$ and one necessarily recovers the results of the CP-invariant theory where ϕ_1 and ϕ_2 mix with each other to form h^0 and H^0, and $\sin\beta\varphi_1+\cos\beta\varphi_2$ is nothering but the pseudoscalar A^0. Thus, in this limit the mixings are as in the CP-invariant theory as is evident from the left panels of each figure. For large $\tan\beta$, however, each Higgs field undergoes certain variations in its compositions. First of all, dominant ϕ_2 composition of the light Higgs boson is easily understandable since the analog of the tree-level Higgs mixing angle (4) approaches $\beta-\pi/2\approx 0$ for large $\tan\beta$ [17]. The remaining component of H_1 comes mainly from ϕ_1 since CP-breaking contributions are small for this eigenvalue [see Eq. (28)]. On the other hand, compositions of H_2 and H_3 are determined from large $\tan\beta$ (dominant ϕ_1 contribution to their CP-even parts) as well as the radiative corrections. As is evident from Eq. (28), in the large $\tan\beta$ regime $M_{13}\sim\sin\gamma\cos\gamma$ and $M_{23}\sim\sin\gamma$ so that (for example) the zeroes of the components of H_2 follow certain combinations of these functional behaviors. The sharp changes in the ϕ_2 and $\sin\beta\varphi_1+\cos\beta\varphi_2$ compositions of H_2 and H_3 at $\gamma=0$ (for large $\tan\beta$) follows from the γ dependencies of M_{13} and M_{23} [see Eq. (28)]. Indeed, variation of the compositions near $\gamma=0$ behaves roughly as $\sin 2\gamma\pm\sin\gamma$ which varies quite fast near the origin.

Until now in Figs. 2–4 we have discussed the CP properties of the eigenstates of the scalar mass-squared matrix equation (19). Now we analyze the γ dependence of the masses of these scalars for identifying their hierarchy. Figure 5 shows the γ dependence of the scalar masses for $\tan\beta=4$ (left panel) and $\tan\beta=30$ (right panel). It is clear that H_1 is the lightest scalar in both cases. Moreover, the small gap (at most $\sim$20 GeV) between M_{H_3} and M_{H_2} in the left

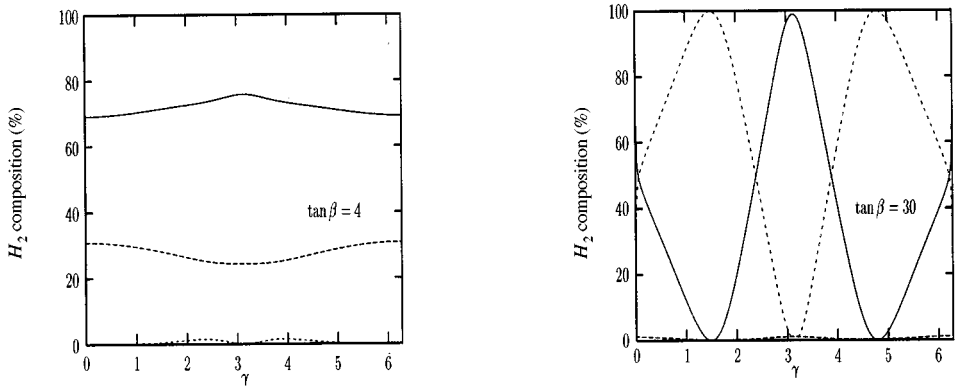

FIG. 3. Percentage composition of H_2 as a function of γ for $\tan\beta=4$ (left panel) and $\tan\beta=30$ (right panel). Here ϕ_1, ϕ_2 and $\sin\beta\varphi_1+\cos\beta\varphi_2$ contributions are $|\mathcal{R}_{21}|^2$ (solid curve), $|\mathcal{R}_{22}|^2$ (dashed curve), and $|\mathcal{R}_{23}|^2$ (short-dashed curve), in percents.

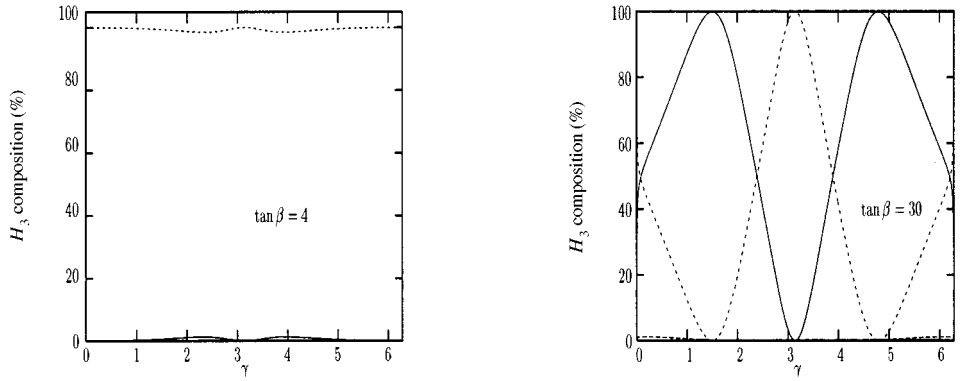

FIG. 4. Percentage composition of H_3 as a function of γ for $\tan\beta=4$ (left panel) and $\tan\beta=30$ (right panel). Here ϕ_1, ϕ_2, and $\sin\beta\varphi_1+\cos\beta\varphi_2$ contributions are $|\mathcal{R}_{31}|^2$ (solid curve), $|\mathcal{R}_{32}|^2$ (dashed curve), and $|\mathcal{R}_{33}|^2$ (short-dashed curve), in percents.

panel is closed in the right panel where H_2 and H_3 are degenerate in mass. This behavior occurs also in the *CP*-conserving case [15,9] due to the large value of $\tan\beta$. One more thing about Fig. 5 is that the masses of H_2 and H_3 are almost completely determined by $\tilde{M}_A=2M_Z$. For instance, for $\tilde{M}_A=10M_Z$, H_2 and H_3 weigh approximately $10M_Z$. Unlike this strong $\tilde{M}_A$ dependence of M_{H_3} and M_{H_2}, mixing among the Higgs scalars and lightest Higgs mass depends mainly on $\tan\beta$. The γ dependence of the masses around $\gamma=\pi$ (especially in the case of $\tan\beta=4$) differ from those at other *CP*-conserving points due mainly to the minimization of the light top squark mass [see Eqs. (16) and (17)]. Finally, one observes that the light Higgs mass is higher than the usual constrained MSSM bounds [18] due to the large value of A_t and relatively small soft top squark masses which is not possible to produce through RGE's (except, possibly, with nonuniversal initial conditions).

From Figs. 2–5 one concludes that the lightest Higgs scalar remains essentially a $CP=+1$ scalar, and the remaining heavy scalars do not possess definite *CP* characteristics. In this sense, the MSSM is seen to accommodate a light $CP=+1$ Higgs boson as in the *CP*-invariant case. In addition, the heavy indefinite *CP* Higgs scalars of the MSSM not only have no correspondent in the standard model (SM) but also are distinguishable from the lightest Higgs boson due to both their masses and *CP* properties. In the next section we shall discuss decay properties of these Higgs scalars to fermions and investigate the deviations from the *CP*-conserving limit.

III. EXAMPLE: DECAYS OF HIGGS SCALARS TO FERMION PAIRS

The form of the scalar mass-squared matrix (19) as well as the mixing matrix $\mathcal{R}$ shows clearly the *CP* violation in the Higgs sector. In general, all parameters of the Higgs sector turn out to depend on these *CP*-violating angles; for instance, $\tan\beta$, masses of scalars, and top squark masses are explicit functions of γ. In this sense the couplings of the Higgs scalars to the MSSM particle spectrum are necessarily modified. Therefore, the *CP*-violating angle γ can show up, for example, in the rates for various collision processes testable at future colliders. As an example, one can consider an e^+e^- collider with sufficiently large center-of-mass energy. In such a collider one of the main Higgs boson production mechanisms is the Bjorken process $Z^*\to ZH_i$. When the center-of-mass energy is varied over a range of values including the masses of the scalars it is expected that the cross section, as a function of the invariant mass flow into the H_i

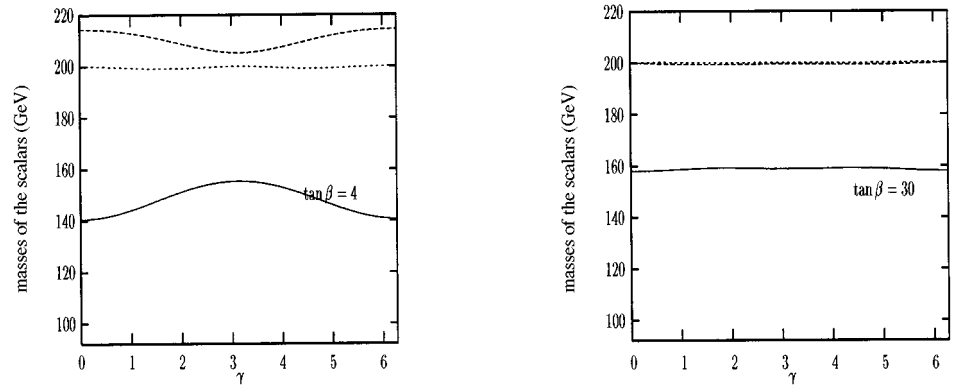

FIG. 5. Masses of the scalars H_i as a function of γ for $\tan\beta=4$ (left panel) and $\tan\beta=30$ (right panel). Here M_{H_1}, M_{H_2}, and M_{H_3} are shown by solid, dashed, and short-dashed curves, respectively. In both panels H_1 is the lightest scalar whose composition is shown in Fig. 2.

TABLE I. Elements of the scalar mixing matrix entering the Feynman rules (32)–(34) for $\tan\beta=4$ and $\gamma=0$. Here $i\,(j)$ runs over $H_i\,(\phi_1,\phi_2,\sin\beta\varphi_1+\cos\beta\varphi_2)$.

$[\mathcal{R}_{ij}(0)]^2$	$i=1$	$i=2$	$i=3$
$[\mathcal{R}_{i1}(0)]^2$	0.31	0.69	0.0
$[\mathcal{R}_{i2}(0)]^2$	0.69	0.31	0.0
$[\mathcal{R}_{i3}(0)]^2$	0.0	0.0	1.0

TABLE II. Elements of the scalar mixing matrix entering the Feynman rules (32)–(34) for $\tan\beta=30$ and $\gamma=0$, with the same convention in Table I.

$[\mathcal{R}_{ij}(0)]^2$	$i=1$	$i=2$	$i=3$
$[\mathcal{R}_{i1}(0)]^2$	0.02	0.98	0.0
$[\mathcal{R}_{i2}(0)]^2$	0.98	0.02	0.0
$[\mathcal{R}_{i3}(0)]^2$	0.0	0.0	1.0

branch, should show three distinct peaks situated at the scalar masses M_{H_i}. Needless to say, in the *CP*-conserving case there would be two peaks instead of three.

We now discuss the couplings of the scalars to fermion pairs in detail. That the scalars H_i are devoid of definite *CP* properties influences their couplings to fermions significantly. Rephasing the fermion fields appropriately one can always make fermion masses real after which the couplings of the scalar H_i to *u*-type quarks, *d*-type quarks, and charged leptons take the form

$$H_i\bar{u}u:(\sqrt{2}G_F)^{1/2}\frac{m_u}{\sin\beta}(\mathcal{R}_{i2}+i\cos\beta\mathcal{R}_{i3}\gamma_5), \tag{32}$$

$$H_i\bar{d}d:(\sqrt{2}G_F)^{1/2}\frac{m_d}{\cos\beta}(\mathcal{R}_{i1}+i\sin\beta\mathcal{R}_{i3}\gamma_5), \tag{33}$$

$$H_i\bar{l}l:(\sqrt{2}G_F)^{1/2}\frac{m_l}{\cos\beta}(\mathcal{R}_{i1}+i\sin\beta\mathcal{R}_{i3}\gamma_5), \tag{34}$$

where one observes that each coupling picks up a γ_5 piece showing its $CP=-1$ content. Moreover, as the Feynman rules above dictate the γ_5 piece is enhanced for large $\tan\beta\,(\cot\beta)$ for *u*-type quarks (*d*-type quarks and charged leptons). To have a quantitative understanding of the effects of γ on the Higgs boson decays to fermion pairs it is convenient to compute the ratio

$$R_{if}=\frac{\Gamma(H_i\to\bar{f}f|\,\gamma\neq0)}{\Gamma(H_i\to\bar{f}f|\,\gamma=0)}=\frac{(\mathcal{R}_{iq})^2(1-4m_f^2/M_{H_i}^2)^{3/2}+a_f^2(\mathcal{R}_{i3})^2(1-4m_f^2/M_{H_i}^2)^{1/2}}{[\mathcal{R}_{iq}(0)]^2[1-4m_f^2/M_{H_i}^2(0)]^{3/2}+a_f^2[\mathcal{R}_{i3}(0)]^2[1-4m_f^2/M_{H_i}^2(0)]^{1/2}}, \tag{35}$$

where $q=2(1)$ and $a_f=\cos\beta(\sin\beta)$ for *u*-type quarks (*d*-type quarks and charged leptons). The argument ''0'' of the quantities in the denominator implies the replacement $\gamma=0$. It is clear that $\Gamma(H_i\to\bar{f}f)$ consists of phase space factors pertinent to both $CP=+1$ and $CP=-1$ cases separately. According to the conventions we apply, for $i=1,2$ $(i=3)$ only the first (second) term survives in the denominator. The *CP*-violating MSSM phase γ not only functions in creating the additional terms in the Feynman rules (31)–(33) but also affects the couplings and masses themselves.

We now perform a numerical computation of R_{if} for the parameter space used up to now. In particular, we concentrate on two cases $f=b$ and $f=c$; that is, we consider *b* and *c* quarks in the computation. Such an analysis will be exhaustive as it covers the cases listed, Eqs. (32)–(34). We start by listing the quantities $[\mathcal{R}_{ij}(0)]^2$ necessary for computing R_{if} in Tables I and II. Below, when speaking about

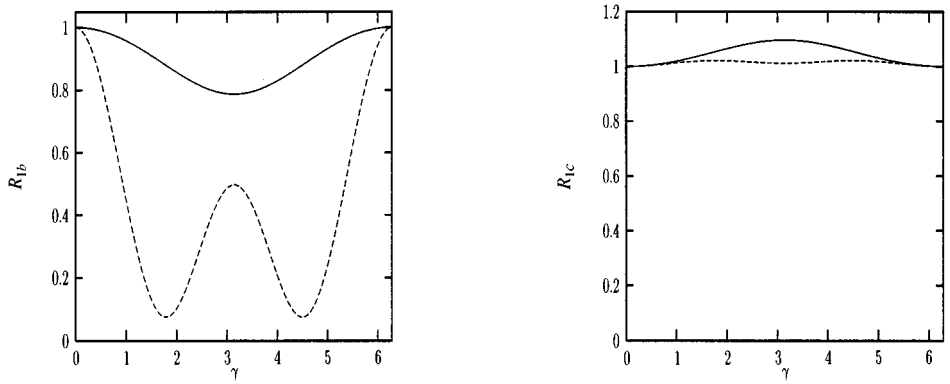

FIG. 6. R_{1b} (left panel) and R_{1c} (right panel) defined in Eq. (34) as a function of γ for $\tan\beta=4$ (solid curve) and $\tan\beta=30$ (dashed curve).

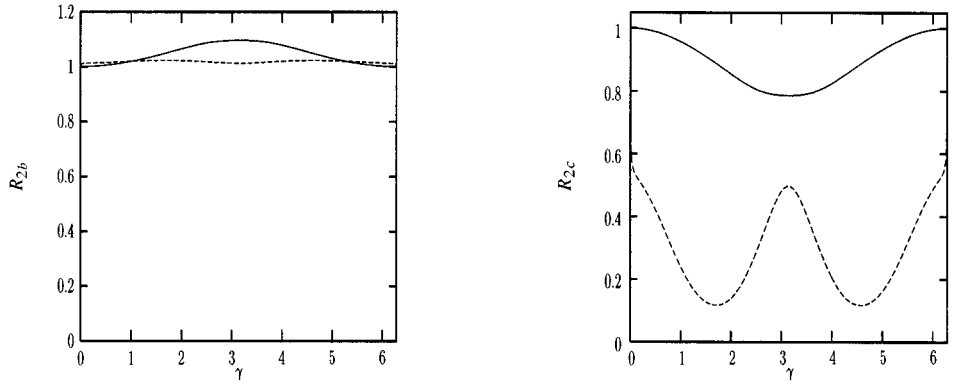

FIG. 7. R_{2b} (left panel) and R_{2c} (right panel) defined in Eq. (34) as a function of γ for $\tan\beta=4$ (solid curve) and $\tan\beta=30$ (dashed curve).

the elements of the mixing matrices for $\gamma=0$ we shall always refer to these tables.

Figure 6 shows the γ dependences of R_{1b} and R_{1c} for $\tan\beta=4$ (solid curve) and $\tan\beta=30$ (dashed curve). Let us first discuss R_{1b} (left panel). As Fig. 2 shows the ϕ_1 composition of H_1 starts with 0.31 at $\gamma=0$ (see Table I) and falls to 0.24 at $\gamma=\pi$. Therefore, R_{1b} falls to $0.24/0.31=0.77$ around $\gamma=\pi$. On the other hand, for $\tan\beta=30 R_{1b}$ obtains a relatively fast variation of R_{1b} with γ. This behavior of R_{1b} follows from its ϕ_1 component in the right panel of Fig. 2, which takes the value of 1.1% around $\gamma=\pi$. Therefore, R_{1b} rises to $0.01/0.02=0.5$ at $\gamma=\pi$ as follows from Table II. On the other hand, from the right panel of the figure one observes that R_{1c} remains around its counterpart in the *CP*-conserving limit. Using Tables I and II and ϕ_2 compositions in Fig. 2 one can easily infer the behavior of R_{1c}. In particular, constancy of the $\tan\beta=30$ curve follows from the constancy of the ϕ_2 composition in Fig. 2 (right panel).

Depicted in Fig. 7 is the dependence of R_{2b} (left panel) and R_{2c} (right panel) on γ for $\tan\beta=4$ (solid curve) and $\tan\beta=30$ (dashed curve). First concentrating on R_{2b}, one observes a slow variation with γ compared to the lightest Higgs boson [Fig. 6 (left panel)]. The behavior of the $\tan\beta=4$ curve simply follows from the ϕ_1 composition of H_2 in Fig. 3 (left panel). However, the flat behavior of R_{2b} for large $\tan\beta$ follows from the complementary behavior of its ϕ_1 and $\sin\beta\varphi_1+\cos\beta\varphi_2$ compositions shown in Fig. 3 (right panel). It is with the $a_b\sin\beta$ factor in Eq. (35) that such a compensation between its opposite *CP* components occur. The variation of R_{2c} follows from the ϕ_2 composition of H_2 in Fig. 3 following the same lines of reasoning used in discussing R_{1b} above.

Finally, Fig. 8 shows the variation of R_{3b} (left panel) and R_{3c} (right panel) with γ for $\tan\beta=4$ (solid curve) and $\tan\beta=30$ (dashed curve). For $\tan\beta=4$, both R_{3b} and R_{3c} remain around unity because of the fact that there is little H-A mixing and $(\mathcal{R}_{33})^2(0)=1$. That R_{3b} remains flat for $\tan\beta=30$ follows from the interplay between its $CP=+1$ and $CP=-1$ components as in R_{2b}. On the other hand, R_{3c} for $\tan\beta=4$ follows simply from its vanishing ϕ_2 and 100% $\sin\beta\varphi_1+\cos\beta\varphi_2$ components in Fig. 4 (left panel). Since the ϕ_2 composition is negligibly small for large $\tan\beta$ (right panel of Fig. 4), variation of R_{3c} is mainly dictated by its $CP=-1$ component (short-dotted curve in the right panel of Fig. 4). For example, $R_{2c}=1$ at $\gamma=\pi$ just due to its 100% composition in Fig. 4.

From the study of the decay rates of the Higgs particles to $b\bar{b}$ and $c\bar{c}$ pairs one concludes that their *CP*-impurity causes significant changes compared to the *CP*-invariant limit. In particular, one notes the enhancement in R_{3c} near the $\gamma=0$ point, which is one order of magnitude above its value in the *CP*-conserving limit.

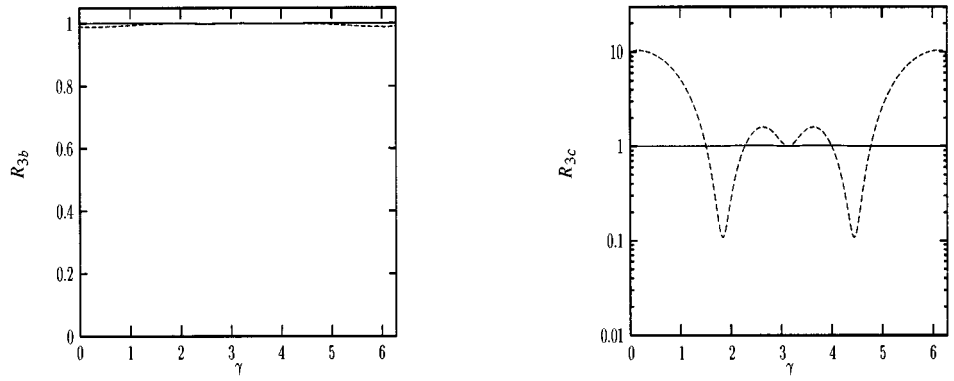

FIG. 8. R_{3b} (left panel) and R_{3c} (right panel) defined in Eq. (34) as a function of γ for $\tan\beta=4$ (solid curve) and $\tan\beta=30$ (dashed curve).

IV. CONCLUSION AND DISCUSSIONS

In this work we have studied the possible effects of supersymmetric *CP*-violating phases on the neutral Higgs scalars of the MSSM. We have adopted the effective potential approximation in computing the radiative corrections and have taken into account only the dominant top quark and top squark loops. We now itemize the main results of the work.

(i) Radiative corrections induce an unremovable relative phase between the two Higgs doublets. This relative phase remains nonvanishing as long as the supersymmetric *CP*-violating phases are finite, and determines the dynamics of the electroweak phase transition [19].

(ii) The $CP=+1$ and $CP=-1$ components of the Higgs doublets are mixed up due to the mixing terms in the scalar mass-squared matrix which (1) are proportional to the relative phase between the two doublets and (2) increase with increasing $\tan\beta$.

(iii) The lightest Higgs scalar remains essentially *CP*-even irrespective of the supersymmetric *CP* phases. Therefore, the MSSM has a light $CP=+1$ scalar as in the *CP*-respecting case which can, however, be distinguished from that of the *CP*-invariant theory, for example, by its reduced decay rate to *bb* pairs.

(iv) As in the *CP*-invariant case, there are two heavy scalars which have (1) definite *CP* quantum numbers for small $\tan\beta$ values and (2) no definite *CP* characteristics for large $\tan\beta$.

(v) The strong mixing between the heavy scalars affect significantly their decay rates to fermion pairs, and such mixings can be important in other collision processes testable at future colliders. Especially the decay rate of the would-be *CP*-odd scalar getes enhanced for $0<\gamma\leqslant\pi/2$.

(vi) The supersymmetric *CP*-violating phases not only cause the creation of *CP*-violating mixings but also modify the couplings and masses compared to ones in the *CP*-invariant case.

In the light of these results one concludes that supersymmetric phases can be useful tools for obtaining manifestations of supersymmetry through their effects on collision and decay processes testable in near future colliders.

ACKNOWLEDGMENTS

It is a pleasure for author to express his gratitude to A. Masiero for highly useful discussions and his careful reading of the manuscript. The author would like to thank T. M. Aliev for helpful discussions.

[1] M. Dugan, B. Grinstein, and L.J. Hall, Nucl. Phys. **B255**, 413 (1985).
[2] S. Dimopoulos, and S. Thomas, Nucl. Phys. **B465**, 23 (1996).
[3] J. Ellis, S. Ferrara, and D.V. Nanopoulos Phys. Lett. **114B**, 231 (1982); W. Buchmüller and D. Wyler, *ibid.* **121B**, 321 (1983); J. Polchinski and M. Wise, *ibid.* **125B**, 393 (1983); F. del Aguila, M. Gavela, J. Grifols, and A. Mendez, *ibid.* **126B**, 71 (1983); D.V. Nanopoulos and M. Srednicki, *ibid.* **128B**, 61 (1983); Y. Kizukuri and N. Oshimo, Phys. Rev. D **46**, 3025 (1992); T. Falk and K.A. Olive, Phys. Lett. B **375**, 196 (1996); T. Falk, K.A. Olive, and M. Srednicki, *ibid.* **354**, 99 (1995).
[4] S.A. Abel and J.M. Frere, Phys. Rev. D **55**, 1623 (1997).
[5] T. Ibrahim and P. Nath, Phys. Rev. D **57**, 478 (1998); **58**, 111301 (1998); M. Brhlik, G.J. Good, and G.L. Kane, *ibid.* **59**, 115004 (1999).
[6] S. Dimopoulos and G.F. Giudice, Phys. Lett. B **357**, 573 (1995); A. Cohen, D.B. Kaplan, and A.E. Nelson, *ibid.* **388**, 599 (1996); A. Pomarol and D. Tommasini, Nucl. Phys. **B488**, 3 (1996).
[7] D.A. Demir, A. Masiero, and O. Vives, Phys. Rev. Lett. **82**, 2447 (1999).
[8] M. Carena and C.E.M. Wagner, hep-ph/9704347; J.M. Cline, M. Joyce, and K. Kainulainen, Phys. Lett. B **417**, 79 (1998); M. Carena, M. Quiros, and C.E.M. Wagner, Nucl. Phys. **B524**, 3 (1998).
[9] H.E. Haber and R. Hempfling, Phys. Rev. Lett. **66**, 1815 (1991); Y. Okada, M. Yamaguchi, and T. Yanagida, Prog. Theor. Phys. **85**, 1 (1991); J. Ellis, G. Ridolfi, and F. Zwirner, Phys. Lett. B **257**, 83 (1991); **262**, 477 (1991); R. Barbieri and M. Frigeni, *ibid.* **258**, 395 (1991).
[10] P. Chankowski, S. Pokorski, and J. Rosiek, Nucl. Phys. **B423**, 437 (1994); A. Dabelstein, *ibid.* **B456**, 25 (1995); Z. Phys. C **67**, 495 (1995); J. Bagger, K. Matchev, D. Pierce, and R. Zhang, Nucl. Phys. **B491**, 3 (1997).
[11] J.A. Casas, J.R. Espinosa, M. Quiros, and A. Riotto, Nucl. Phys. **B436**, 3 (1995); M. Carena, J.R. Espinosa, M. Quiros, and C. Wagner, Phys. Lett. B **355**, 209 (1995); M. Carena, M. Quiros, and C. Wagner, Nucl. Phys. **B461**, 407 (1996); H.E. Haber, R. Hempfling, and A. Hoang, Z. Phys. C **75**, 539 (1997).
[12] R. Hempfling and A. Hoang, Phys. Lett. B **331**, 99 (1994); R.-J. Zhang, *ibid.* **447**, 89 (1999).
[13] S. Heinemeyer, W. Hollik, and G. Weiglein, hep-ph/9812472.
[14] A. Pilaftsis, Phys. Rev. D **58**, 096010 (1998); Phys. Lett. B **435**, 88 (1998).
[15] J. F. Gunion, H. E. Haber, G. Kane, and S. Dawson, *The Higgs Hunter's Guide* (Addison-Wesley, New York, 1990).
[16] M. Sher, Phys. Rep. **179**, 273 (1989).
[17] H. E. Haber, hep-ph/9505240.
[18] J. R. Espinosa, Surv. High Energy Phys. **10**, 279 (1997).
[19] K. Funakubo, Prog. Theor. Phys. **101**, 415 (1999); M. Laine and K. Rummukainen, Nucl. Phys. **B545**, 141 (1999).